CHARACTERIZING AN ALTERNATIVELY SPLICED VARIANT OF CHEMOKINE RECEPTOR 2 IN PAINFUL DIABETIC NEUROPATHY

JUSTINE SOLTYS
LEI YU (FACULTY ADVISOR)

✷ ABSTRACT

Prior research efforts have demonstrated a link between neuroinflammation and the progression of Painful Diabetic Neuropathy (PDN), a chronic cascade of nerve damage that presents as tingling, numbness, hypersensitivity to touch, or intense pain. Current treatments are focused on pain management, serving to temporarily mask these symptoms without repressing or slowing nerve damage. The chemokine-receptor system has been closely studied for its role in perpetuating neuropathic pain, although its precise mechanistic involvement remains unclear due to the network's complexity. Because of its likely role in regulating neuropathic pain, targeting CCR2 may be the key to effective treatment of PDN.

Alternative splicing of CCR2 leads to two distinct isoforms with different C-terminus sequences, CCR2A and CCR2B. The present study was intended to differentiate between these isoforms through specific primer design, selection of optimized pairs, RT-PCR, and amplicon sequencing to verify the PCR products. However, the study has revealed a third, previously unreported isoform, CCR2C, due to evidence of alternative splicing and both the absence and insertion of parts of A and B. In the long term, we predict that the relationship between CCR2's alternatively spliced transcript variants will lead to a distinct pattern of isoform prevalence in individuals suffering from PDN. Discerning the genetic profiles of patients with PDN and healthy individuals will clarify the complex mechanism driving CCR2's intracellular interactions and offer more effective therapeutic options.

1 INTRODUCTION

PAINFUL DIABETIC NEUROPATHY

Painful Diabetic Neuropathy (PDN) gives rise to several types of peripheral nerve damage but most frequently affects the feet in a pattern of distal-to-proximal severity. During disease progression, the extremities are more severely impacted than the midline of the body, which models the branching peripheral nervous system. Those neurons comprised of the longest axons exhibit increased exposure due to their size and distribution, thus sustaining the brunt of the damage.[11] As the sensory nerves are affected, individuals may experience numbness tingling, or a loss of reactivity to sensations like temperature, pain, or touch. Damage to the motor nerves causes hyperalgesia (enhanced pain sensitivity) and allodynia (hypersensitivity to neutral stimuli often felt as a stabbing pain).[20] The incidence of PDN within diabetes ranges between 10–26%, reflecting differences among sample populations.[2]

In individuals with PDN, a number of related metabolic and vascular factors are implicated in the onset of nerve damage. Nerve damage stimulates the infiltration of macrophages, leading to an increase in the number of pro-inflammatory cytokines circling throughout the body. Clinical studies involving diabetic neuropathic (DN) subjects with and without pain demonstrate that groups experiencing PDN have higher inflammation markers and increased cytokine concentration. The neuroinflammatory and immune responses are thus heightened and contribute to the development of neuropathic pain.[1]

Several factors are believed to contribute to the pain mechanism of PDN; as a result, current treatment options are decidedly limited. Glycemic

control, anticonvulsants, antidepressants, and opiates are meant to assuage pain and other symptoms related to PDN, but fail to restore nerve function.[13] Tightened glycemic control lowers the blood sugar levels in an effort to reduce the risk of hyperglycemia, a causative factor in neuropathy. While this practice has displayed some success in slowing the progression of PDN, it does not alleviate nerve pain, and other drugs vary in the consistency of their results.[6] Individuals suffering from PDN continue to live with nerve pain, loss of sensation, and the risk of limb amputation. Because of this, there is still a pressing need to understand how PDN manifests and to develop effective therapeutic options that treat PDN directly.

THE ROLE OF CCR2 IN PDN

The chemokine-receptor network has been widely implicated in both inflammatory pain conditions and neuropathic pain. Chemokines are a subset of cytokines responsible for attracting white blood cells to sites of inflammation through induced chemotaxis. C-C motif chemokine ligand 2 (CCL2) binds to C-C motif chemokine receptor type 2 (CCR2), with a high level of affinity. Their interaction at the monocyte membrane is represented locally by a CCR2/CCL2 axis, creating a gradient with increasing monocyte concentration in the direction of inflammatory sites. As a result of its influence on the migration of white blood cells, CCR2/CCL2 signaling guides a number of key protective and destructive responses of the immune system (Hughes et al., 2018).

CCR2 is known to have two alternatively spliced transcript variants, CCR2A and CCR2B, which differ in the lengths of their cytoplasmic tails at the C-terminus. CCR2A consists of three exons, while CCR2B has an additional exon which is unique to that isoform. Alternative splicing describes the process wherein a single gene is assembled through different regulatory mechanisms to encode for multiple proteins. The precursor to mRNA, pre-mRNA, may contain exons that are omitted, shortened, or have higher sequence conservation as compared to other examples of mature mRNA. Conventional chemokine receptors, a family of chemokine-binding surface molecules, are often subject to alternative splicing. Like variants of CCR2, chemokine receptors CCR9, CXCR3, and CXCR4 have been specifically associated with changes in ligand-binding or signaling properties, which supports the idea that isoforms of CCR2 maintain altered properties.[5,18] G-protein coupled receptors, such as CCR2, are dependent on the amino acid sequence of their C-terminal domain for intracellular signaling. Therefore, it is likely that functional differences between CCR2A and CCR2B will lead to their distinct signaling roles, despite the presence of a shared extracellular protein motif.[18]

Preclinical studies have demonstrated the involvement of CCR2 and CCL2 in the pathophysiology of neuropathic pain, with these models suggesting that CCR2-antagonists can reduce painful symptoms.[1] A 2013 AstraZeneca study sought to evaluate the efficacy and safety of the drug AZD2423 as a novel CCR2-antagonist in subjects with PDN.[9] CCL2 plasma levels increased in a dosage-dependent manner, and mean monocyte levels declined by approximately 27%, indicating that AZD2423 interacted with its intended target, CCR2. However, AstraZeneca's study failed to show that AZD2423 alleviated primary and most secondary pain variables with greater efficacy than the placebo. We suggest that AZD2423 was found to be an ineffectual clinical treatment because it was not designed to cater to the distinct structural components of CCR2. To improve the efficacy of medications like these, our research has focused on understanding the levels of CCR2 variants in populations that suffer from PDN. Stratifying drug treatment based on the expression ratio of individuals' CCR2 isoforms may enhance the efficacy of therapeutics in mitigating pain. From this data, we aim to decode the role of alternatively spliced CCR2 variants in the incidence of PDN and pathophysiology of neuropathic pain. We initially performed amplicon sequencing of PCR products to analyze the genetic variation in a specific region and confirm their genomic contents. Unexpectedly, we found evidence of additional alternative splicing sites, which implies the existence of a third isoform,

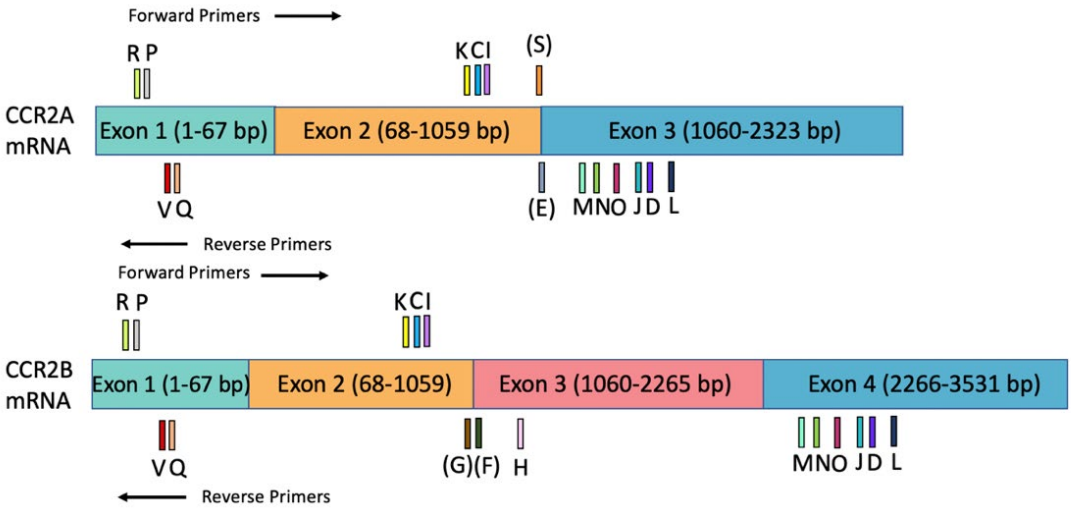

FIGURE 1: *A comparison of CCR2's previously recorded isoforms, which depicts that CCR2A lacks an additional exon. Exons 1 and 2 represent a conserved region between the variants, 67 base pairs (bp) and 992 bp long, respectively. The last exon is 2 bp longer in CCR2B than in CCR2A. Primers listed within parentheses are situated at junctional sites, thus spanning two exons.*

CCR2C. The present study identifies CCR2 and characterizes its presumed functional relationship with CCL2 following RT-PCR, gel electrophoresis, and analysis of amplicon sequencing results.

2 METHODOLOGY

Blood samples were obtained from 17 donors; 11 were from individuals with diabetes and/or PDN, and 6 from individuals who were healthy. Each subject provided three 10 mL collection tubes of blood. We assigned each subject a letter from A through Q and marked the blood samples with their corresponding letter. Because monocytes are a direct contributor to the neuroinflammatory model of DN, we were primarily interested in the buffy coat and plasma, as these components have the highest concentrations of white blood cells. We treated the collection tubes of buffy coat with RNAlater, a stabilizing reagent that inactivates RNases and maintains the integrity of the RNA.

We extracted RNA from the whole blood samples on the date of their arrival in an effort to reduce degradation. First, we distributed the 5 mL of blood that was initially set aside into 200 µL test tubes, using the standard protocol from the NEB Monarch Total RNA mini-kit. The whole blood samples were lysed upon mixing with a 2X Monarch DNA/RNA Protection Reagent Concentrate. The whole blood RNA was then distributed into aliquots and stored at -80° C until further processing.

HEPARINASE TREATMENT

Because of the scarcity of the buffy coat layer and its viscosity, we experienced challenges extracting quantifiable levels of RNA, thus requiring that cDNA production in Reverse Transcription (RT) be maximally optimized. To improve cDNA yield, Heparinase I, a polysaccharide lyase, was added to the RNA before RT to cleave Heparin, an anticoagulant often used in blood sample processing. Heparin tends to be used to prevent the clotting and clumping of cells, but it also inhibits the activity of the reverse transcriptase enzyme. Test tubes were prepared containing RNA, Heparinase I, buffer, $MgCl_2$,

and RNAse inhibitor (New England BioLabs reagents). Some of these reagents were added in half-volumes or less, with the remainder pipetted into the test tube after it was placed in a PTC-100 machine at 25°C for a two hour-long incubation period.

RT-PCR AND GEL ELECTROPHORESIS

In designing isoform-specific primer pairs, we first developed primers which could distinguish CCR2A from CCR2B by binding to the regions unique to each variant. A two-letter nomenclature was developed, with the first letter referencing the forward primer and the second corresponding to the reverse. Because they are complementary to sequences on CCR2B-Exon 3, reverse primers F, G, and H, in combination with a forward primer, can only successfully bind to and amplify CCR2B during PCR. However, conserved primer pairs able to bind to both CCR2A and CCR2B might still selectively amplify only a single variant, depending on the resulting size of the PCR product. Any product greater than 1,000 base pairs (bp) long is generally longer than the polymerization rate of the Taq polymerase enzyme can accommodate under standard PCR extension times. In each cycle of PCR, 1 minute generally allows for up to 1 kb of the amplicon to be amplified, thus eliminating larger products. For example, primer pair IN was previously confirmed by the author as a reliable CCR2A primer combination, yielding a PCR product 267 bp long. IN can also bind to CCR2B, but the presence of the third exon creates an unlikely PCR product that stretches 1,464 bp; there is no current experimental data to support its specificity to CCR2B. CH and IH have both worked equally well as CCR2B-specific primer sets, likely because they bind to locations sitting relatively near each other. CH and IH isolate 309 and 222 bp PCR products in CCR2B, respectively. Both primer combinations PQ and VR have been validated as CCR2 internal controls because they bind to locations within the conserved region shared by each of the transcript variants, Exons 1 and 2, producing identical amplicons in each.

Following heparinase treatment, buffer, $MgCl_2$, dNTPs, Random Hexamers, Oligo dT, and Reverse Transcriptase were incorporated into the RNA solute (SUPPLEMENTAL TABLE 1). The precise volumes of the reagents for PCR (SUPPLEMENTAL TABLE 2) tended to be more flexible because 1 to 3 primer sets can be tested against a patient sample, which slightly alters the volume of water added to bring the master mix to 20 µL. The annealing step of PCR was consistently run at 54°C for 30 seconds. To make the agar component of a gel, we added 0.35 g of Agarose and 25 mL of 1X TBE to a 50 mL flask and heated repeatedly until the solution was completely clear, with no pellets of agarose visible. The solution was poured into the tray of the gel box, solidified, and run at approximately 110 Volts until the bands travelled two-thirds of the way to the opposite end of the gel. After being removed from the basin, the gel was stained with Ethidium Bromide for 20–30 minutes and photographed.

All primers were designed using AmplifX and Oligo 7 software and ordered through Integrated DNA Technologies. We carried out RT-PCR and gel electrophoresis for 12 primers pairs which had previously produced bands for CCR2A and CCR2B using reference RNA: CD, CJ, CL, CM, CN, CO, ID, IJ, IL, IM, IN, and IO. Amplicon sequencing was performed by GeneWiz, using next generation sequencing technology.

3 RESULTS

During our initial testing, we performed RT-PCR and gel electrophoresis in order to establish reliable sets of primers for further quantification of CCR2 variants in patient samples. RT generated complementary DNA (cDNA), a copy of mRNA used as a template for PCR. In the following step, CCR2 variant-specific primer pairs amplified CCR2A and CCR2B, creating millions of copies. These PCR products were evaluated using gel electrophoresis to confirm that their lengths matched the determined amplicon size of each primer combination. While gel electrophoresis is a reliable visual tool, amplicon sequencing was needed to positively identify each DNA sequence as a product of either CCR2A or CCR2B. Each lane of FIGURE 2 represents the contents of a CCR2A-specific primer combination. Clear bands can be seen at the expected amplicon lengths for all primer combinations except CF, whose attributed PCR products were eliminated from the in-

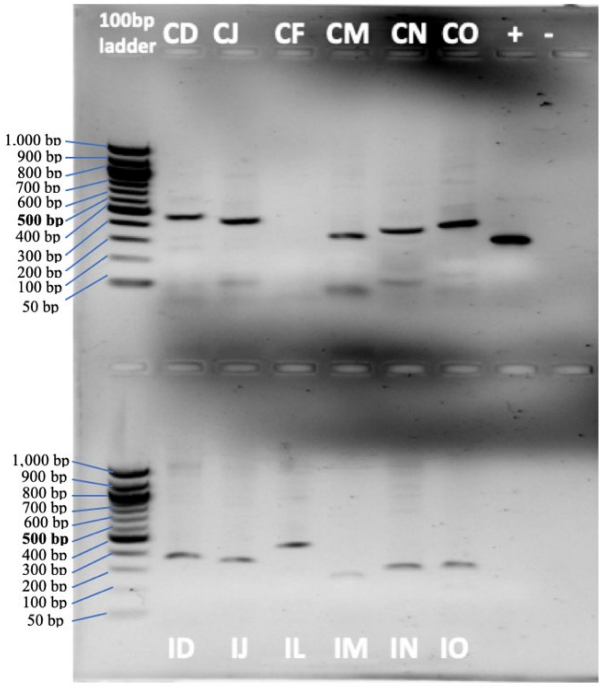

FIGURE 2: *Gel depicting CD, CJ, CF, CM, CN, CO, ID, IJ, IL, IM, IN, and IO primer bands with plasma-extracted RNA as the template. Each band corresponds to its "expected length in CCR2A" (TABLE 1), though no band appears for CF. Primer pair CF may have been unsuccessful at binding to the cDNA if its melting temperature was outside of the range of the other sets, or within a region of secondary structure.*

Pair	Band length	Expected Length in CCR2A (bp)
CD	450	453
CJ	425	422
CM	300	311
CN	350	360
CO	370	372
ID	370	360
IJ	330	329
IL	420	420
IM	250	218
IN	270	267
IO	270	279

TABLE 1: *Expected primer pair lengths relative to isoform CCR2A, along with their approximate experimental band lengths determined from the published isoform's DNA sequence.*

ventory stored for amplicon sequencing. Primer dimers appeared in all forward primer C-containing gel lanes below the 100 bp mark, often seen in Ethidium bromide-stained gels in the 30-50 bp range, resulting from primers attaching to each other.

We also ran RT-PCR for other combinations that could be attributed to CCR2B (gel not pictured). There were a few instances of multiple bands in the case of CD, IM, IN, and CJ, which proved unusual due to the 1-minute cycle extension time during PCR, but not impossible for CCR2B-specific PCR products of approximately 1,000 bp. In theory, all four sets could bind to both variants, CCR2A and CCR2B. For the samples that presented the expected base pair lengths, our next step was to confirm these results with amplicon sequencing. Following high-throughput marker gene analysis, the amplicon sequences were read and totaled, representing a match to a predicted primer pair–generated PCR sequence.

A major discrepancy was seen in the produced sequence alignment for primer set CD, which illustrated a missing piece of variant CCR2A nearly 300 base pairs long. Amplicon sequencing of CD yielded four significant sequences which we referred to by their lengths in base pairs. 190, 356, and 208 were a match to other chromosomes, while 115 corresponded to an ~180 gel band after accounting for the size of the forward and reverse primers. However, 115's alignment to CCR2A was clearly dis-

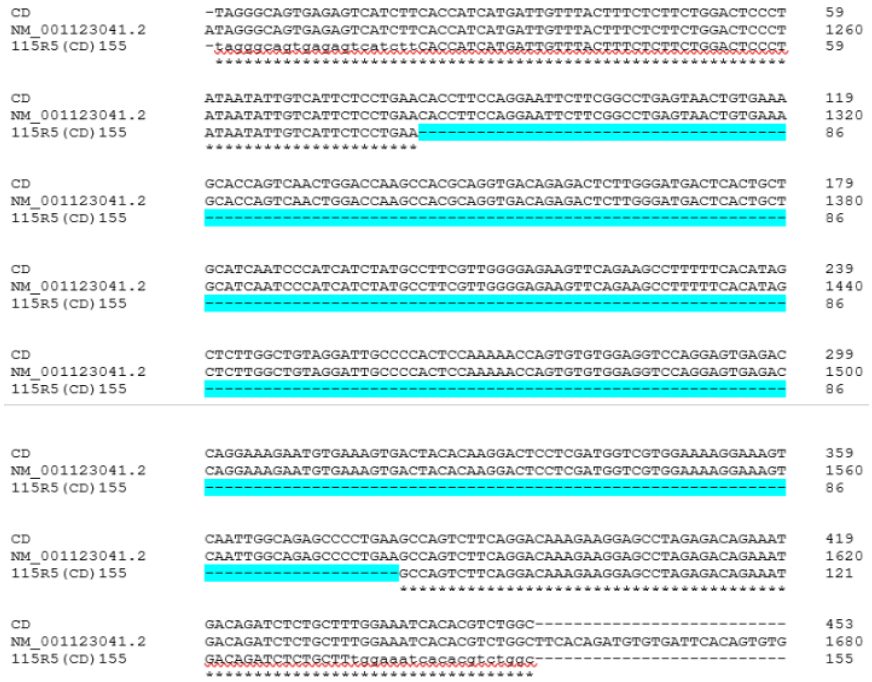

FIGURE 3: *The spaces highlighted in blue indicate expected base pairs absent from amplified CD 115, in relation to CCR2A. This missing sequence does not display the 5'-GT AG-3' sequence characteristic of intron removal, as a result of alternative splicing.*

rupted, though there was no immediate evidence of alternate splicing against CCR2B (FIGURE 3). This finding is highly irregular, considering that the primer pair must have successfully bound to the cDNA for a PCR product of any length to have been amplified.

Primers CN, IN, CD, CJ CM, CO, ID IJ, IL, and IM produced segments that matched their expected CCR2A lengths. However, a few amplified fragments attributed to CN, IN, and ID were only partial matches to the entire expected sequence. For each primer combination, we analyzed the alignment of the sequences as compared the expected amplification on either CCR2A, CCR2B, or both and generated dot matrix plots (not pictured) to better visualize the accuracy of the predicted to the actual amplification. At this stage, we intended to identify the major sequences amplified, determine the primer sequences which might need to be trimmed or excluded from future analysis, and differentiate between those that were exclusive to either CCR2A or CCR2B.

Of IN's two significant sequences, IN 78 corresponded to various human and primate sequences other than CCR2, but IN 364 was an imperfect match to CCR2B, displaying possible evidence of alternative splicing due to the presence of multiple GT-AG splicing sites (FIGURE 4). IN 364 exhibited other unexpected alignments, including a portion of CCR2B's third unique exon situated within a region of CCR2A, as shown in FIGURE 5.

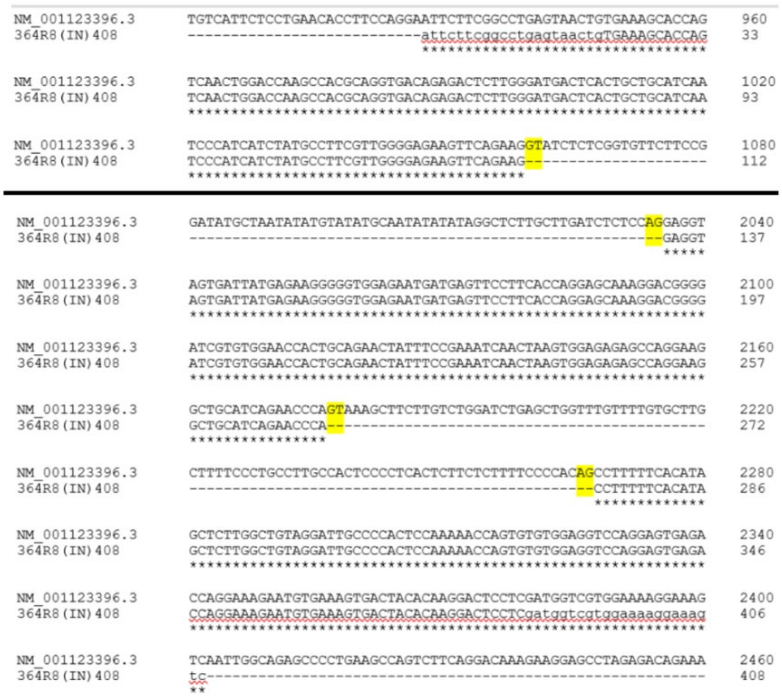

FIGURE 4: *This alignment of IN 364 to CCR2B appears to be the result of alternate splicing, as evidenced by the yellow GT-AG sequences.*

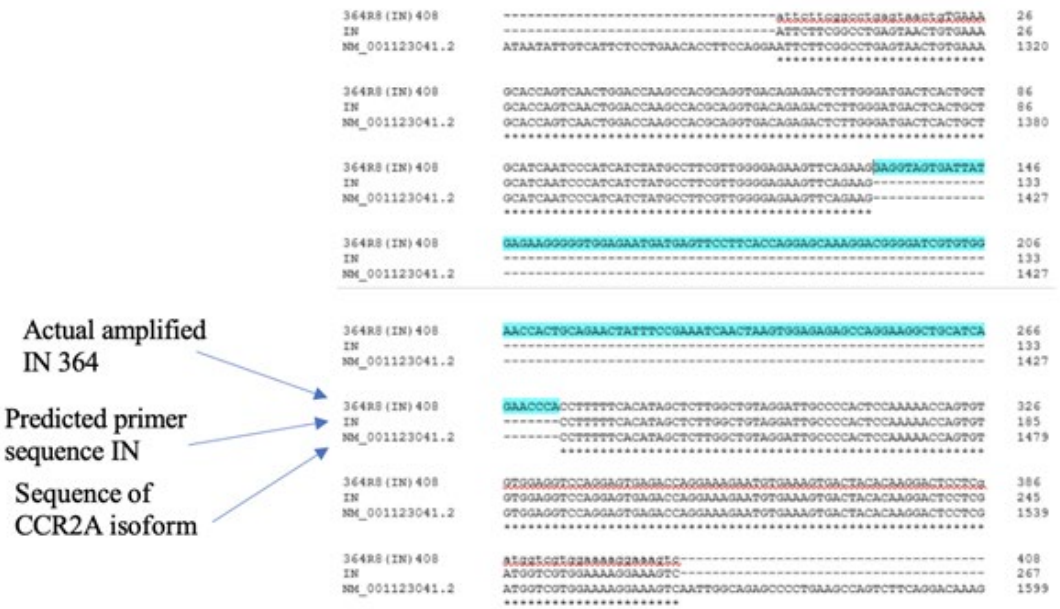

FIGURE 5: *The base pairs highlighted in blue indicate a portion of the amplified sequence IN 364 that was not part of the predicted CCR2A sequence.*

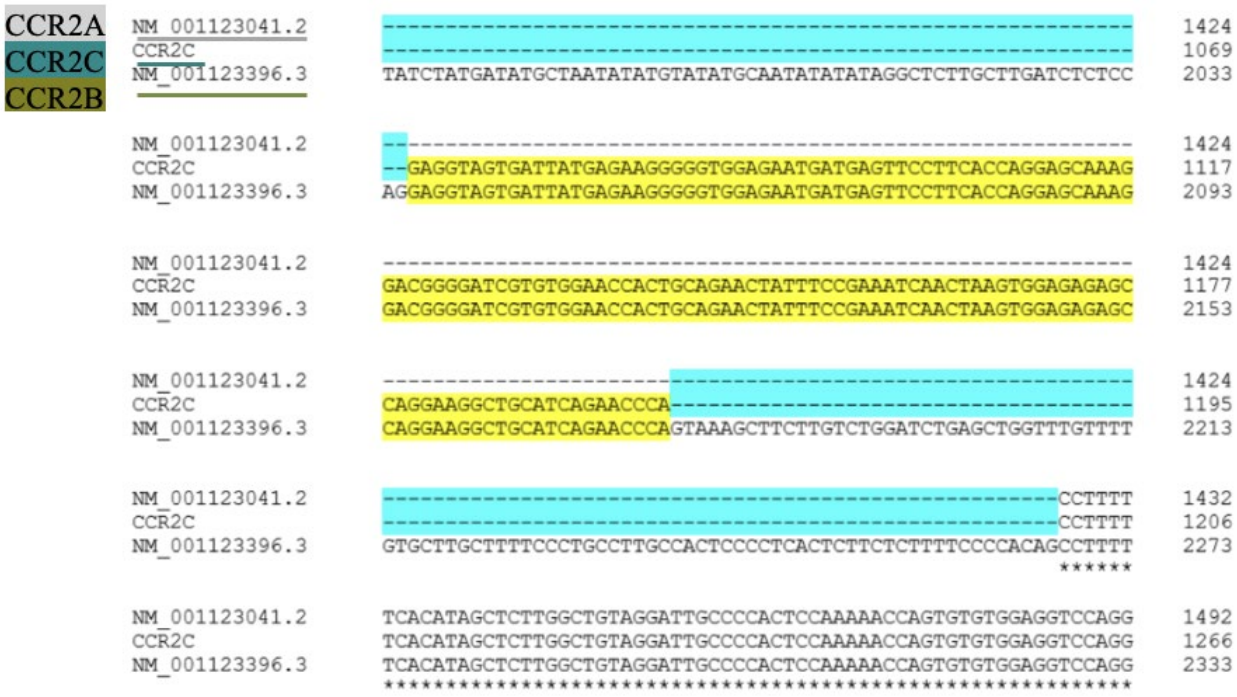

FIGURE 6: *In this region of the IN 364 sequence, the gene behaved primarily like CCR2A, though the blue highlights base pairs which should be present, and the yellow highlights a portion of CCR2B unexpectedly included in the alignment. At the left is the proposed third isoform CCR2C. This alignment suggests that the only difference between CCR2C and CCR2B is the contiguous nature of Exon 3 in CCR2B, and the removal of two introns from Exon 3 in CCR2C.*

FIGURE 6 identifies both an absent sequence from CCR2A and the addition of part of CCR2B, producing a drastically changed sequence, shortened from the presence of additional splicing sites and yet incorporating parts of CCR2B-Exon 3.

4 DISCUSSION

Collectively, the sequence alignments comparing CD 115 and IN 364's amplified products to our predicted sequences provide strong evidence of a third variant of the CCR2 gene. From our preliminary results, we observed unexpected alternative splicing and absent portions of the targeted isoform, revealing the existence of CCR2C. Due to the distinct inclusion of Exon 3 in CCR2B and parts of the same exon in CCR2C, the amino acid sequences of their C-terminus signaling region will be changed, likely causing functional differences in intracellular signaling to arise. CCR2C may have significance in the quantification of isoform expression levels between normal and diabetic patients. We propose that individuals' expression profiles will translate to CCR2-antagonist responsiveness for AZD2423 and contribute to a genetic stratification approach for other PDN treatments.

CCR2's coding frame presents a long peptide with the signature motif of an integral membrane protein and a transmembrane domain. Alternative splicing shifts the translational frame, causing each of the three variants to represent a different reading frame. Despite lacking a fourth exon, CCR2A's open reading frame is longer than CCR2B's; thus, the variant maintains a longer carboxy terminal tail. CCR2C's cytoplasmic tail is greatly truncated, suggesting that the open reading frame ends a few amino acids into the C terminal (FIGURE 7).

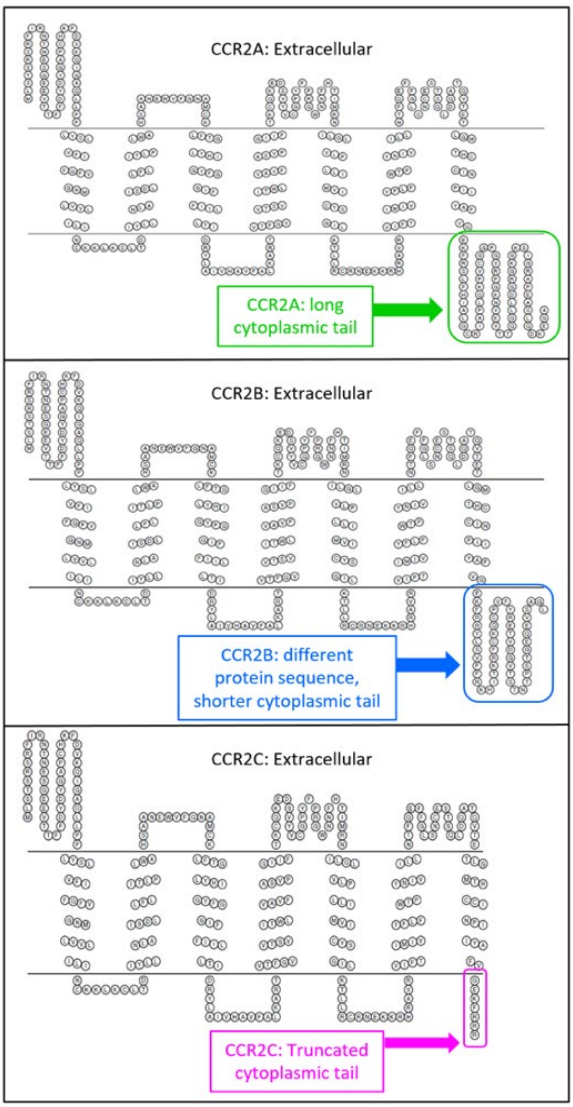

FIGURE 7: *Contrasts the extracellular protein sequences of CCR2's variants. The size of the protein's cytoplasmic tail is a function of the reading frame's positioning, which determines the amino acids encoded by the gene.*

The shortness of its carboxy tail could result in an effectively nonfunctional CCR2C isoform, the equivalent of a nonsense or stop mutation. CCR2C has a transmembrane and extracellular domain which appear identical to CCR2A and CCR2B, so CCR2C may become a sink, soaking up peptides or ligands that activate normal receptors. CCR2C would be similarly able to bind to CCL2, but this interaction would not trigger an active, intracellular response, reducing signal transduction.

Assuming that CCR2C has the same 5′ sequence as CCR2A and CCR2B, either PQ or VR should, in theory, be able to target CCR2 equally well. As a result, the amplification of sequences using primers PQ and RV represents the total level of CCR2 expression, though there may be other undiscovered isoforms of the CCR2 gene, which do not possess complete Exon 1 similarity. The next step with regards to primer design would be to synthesize primer sets that can reliably differentiate between CCR2B and CCR2C so that each isoform can be quantified separately. The PCR product of CCR2C should be shorter than CCR2B because of the removal of two introns, allowing us to discern between the variants. Two bands may be amplified, but given a distinctive difference in their lengths, gel electrophoresis bands should be clearly attributed back to CCR2B or CCR2C. We intend to determine CCR2 expression levels in order to understand the role of its isoforms in perpetuating nerve damage, pain, and/or loss of peripheral sensation.

Although we began this study to identify ratio differences in CCR2A/B in patient populations, amplicon sequencing results revealed distinct differences in sequences recovered from PCR, pointing to a third variant of CCR2. Alternative splicing of pre-mRNA thus establishes three isoforms: A, B, and C. As a target of interest in prominent inflammatory and neuropathic pain conditions, antagonists of CCR2, such as AZD2423 have been clinically tested with some level of success.[9] However, CCR2 variant expression may offer insight into drug responsiveness, serving as a biological marker of PDN treatment efficacy■

5 ACKNOWLEDGEMENTS

I would like to thank Dr. Lei Yu for his tireless support and guidance. It is because of his far-reaching intellectual curiosity that I have had the privilege of working on this incredibly fulfilling project and have learned so much. I would also like to extend my thanks to fellow Neuroinflammation lab members Anika Patel and Madhuri Achanta, who not only contributed data, but also carried the enthusiasm to follow scientific leads like true detectives.

6 REFERENCES

[1] Abbadie, C., et al. (2003). Impaired Neuropathic Pain Responses in Mice Lacking the Chemokine Receptor CCR2. *Proceedings of the National Academy of Sciences of the United States of America*, 100(13), 7947–7952.

[2] Abbott CA, Malik RA, van Ross ER, Kulkarni J, Boulton AJ. Prevalence and characteristics of painful diabetic neuropathy in a large community-based diabetic population in the U.K. *Diabetes Care*. 2011;34:2220–2224.

[3] Biolabs, New England. "Guidelines for RNA Purification from Whole Blood." *NEB*
WWW.NEB.COM/TOOLS-AND-RESOURCES/USAGE-GUIDELINES/GUIDELINES-FOR-RNA-PURIFICATION-FROM-WHOLE-BLOOD

[4] Callaghan, B., Cheng, H., Stables, C., Smith, A., & Feldman, E. (2011). Diabetic Neuropathy: Clinical Manifestations and Current Treatments. *Lancet Neurology*, *11*(6), 521–534.

[5] Charo, I. F., Myers, S. J., Herman, A., Franci, C., Connolly, A. J., & Coughlin, S. R. (1994). Molecular cloning and functional expression of two monocyte chemoattractant protein 1 receptors reveals alternative splicing of the carboxyl-terminal tails. *Proceedings of the National Academy of Sciences*, *91*(7), 2752–2756.

[6] Datta, I., Bhadri, N., Shahani, P., Majumdar, D., Sowmithra, S., Razdan, R., & Bhonde, R.(2017). Functional recovery upon human dental pulp stem cell transplantation in a diabetic neuropathy rat model. *Cytotherapy*, *19*(10), 1208–1224.

[7] Hughes, C. E., & Nibbs, R. J. (2018). A guide to chemokines and their receptors. *The FEBS Journal*, *285*(16), 2944–2971.

[8] Johnson, M. L., et al. (2003). Heparinase Treatment of RNA before Quantitative Real-Time RT-PCR. *BioTechniques*, 35(6), 1140–1144.

[9] Kalliomäki, J., Jonzon, B., Huizar, K., O'malley, M., Andersson, A., & Simpson, D. (2012). Evaluation of a novel chemokine receptor 2 (CCR2)-antagonist in Painful Diabetic Polyneuropathy. *Scandinavian Journal of Pain*, *4*(2), 77–83.

[10] Kaur, S., et al. (2011). Painful diabetic neuropathy: an update. *Annals of neurosciences*, 18(4), 168-75.

[11] Morales-Vidal S, Morgan C, McCoyd M, Hornik A. Diabetic peripheral neuropathy and the management of diabetic peripheral neuropathic pain. *Postgrad Med*. 2012;124:145–153.

[12] NanoDrop Technologies. *260/280 And 260/230 Ratios Technical Support Bulletin*. *260/280 And 260/230 Ratios Technical Support Bulletin*, NanoDrop Technologies, Inc, 2007.
HTTPS://WWW.BIO.DAVIDSON.EDU/PROJECTS/GCAT/PROTOCOLS/NANODROP_TIP.PDF

[13] Nathan, D. M., and DCCT/EDIC Research Group. (2014). The diabetes control and complications trial/epidemiology of diabetes interventions and complications study at 30 years: overview. *Diabetes care* 37(1), 9-16.

[14] Sloan, G., Shillo, P., Selvarajah, D., Wu, J., Wilkinson, I. D., Tracey, I., … Tesfaye, S. (2018). A new look at painful diabetic neuropathy. *Diabetes Research and Clinical Practice*, *144*, 177–191.

[15] Totsch, S. K., and Sorge, R. E. (2017). Immune System Involvement in Specific Pain Conditions. *Molecular Pain*, 13.

[16] Tsai, Richard. "DNA Purification Using Buffy Coat." *Inside Biobanking*, 8 Jan. 2015
WWW.THERMOFISHER.COM/BLOG/BIOBANKING/DNA-PURIFICATION-USING-BUFFY-COAT/

[17] Van Acker, K., et al. (2009). Prevalence and Impact on Quality of Life of Peripheral Neuropathy with or without Neuropathic Pain in Type 1 and Type 2 Diabetic Patients Attending Hospital Outpatients Clinics. *Diabetes & Metabolism*, 35(3), 206–213.

[18] Wong, L.-M., Myers, S. J., Tsou, C.-L., Gosling, J., Arai, H., & Charo, I. F. (1997). Organization and Differential Expression of the Human Monocyte Chemoattractant Protein 1 Receptor Gene. *Journal of Biological Chemistry*, *272*(2), 1038–1045.

[19] Yoon, J. W., and Jun, H. S. (2005). Autoimmune Destruction of Pancreatic Beta Cells. *American Journal of Therapeutics*, *12*(6), 580–591.

[20] Zhu, T., Meng, Q., Ji, J., Zhang, L., & Lou, X. (2017). TLR4 and Caveolin-1 in Monocytes Are Associated with Inflammatory Conditions in Diabetic Neuropathy. *Clinical and Translational Science*, *10*(3), 178–184.

Justine Soltys is a senior in the School of Arts and Sciences, majoring in Molecular Biology and Biochemistry, with a minor in history. Her research sits within the intersection between inflammation and neuropathic pain, under the guidance of Dr. Lei Yu at the Center for Alcohol Studies. At the Yu lab, she studies the isoform expression of CCR2's alternatively spliced variants as a potential biomarker and treatment target in Painful Diabetic Neuropathy. In the summer of 2021, she interned with the Discovery Toxicology- Non-Clinical Research and Development division of Bristol Myers-Squibb to investigate calcium dysregulation of ryanodine receptor 2 (RYR2) in catecholaminergic polymorphic ventricular tachycardia (CPVT). The common thread underlying both projects is pharmacogenetics, unique drug response influenced by genetic variations. After her undergraduate years, she hopes to obtain a PhD and contribute to pharmacology discovery and development. For questions, please contact her at:
JUSTINE.SOLTYS@RUTGERS.EDU

7 SUPPLEMENTAL TABLES

REAGENT	PER TUBE (µL)
DH2O	10.7*
BUFFER	2.0
DNTP	0.4
TAQ POLYMERASE	0.1
CDNA	6.0
FORWARD PRIMER	0.4
REVERSE PRIMER	0.4
TOTAL	**20.0 µL**

SUPPLEMENTAL TABLE 1: *RT reagent table, establishing the standard reagent volumes per reaction.*

REAGENT	PER TUBE (µL)
BUFFER	2.5
$MgCl_2$	2.25
DNTP	10
RANDOM HEXAMERS	1.25
OLIGO DT	1.25
REVERSE TRANSCRIPTASE	1.25
TOTAL	**18.5 µL**

SUPPLEMENTAL TABLE 2: *PCR reagent table, illustrating the variability of reagent ratios.*

**Can change relative to the volume of cDNA and number of primer sets per reaction tube.*

Name of Primer	Sequence	Exon Location	Forward or Reverse Primer
C	5'TAGGGCAGTGAGAGTCATCTT 3'	2	Forward
D	5'GCCAGACGTGTGATTTCCA 3'	3	Reverse
E	5'GCTATGTGAAAAAGGCTTCTGA 3'	2 and 3 (Junction)	Reverse
F	5'AACACCGAGAGATACCTTCTG 3'	2 and 4 (Junction)	Reverse
G	5'CACCGAGAGATACCTTCTGAA 3'	2 and 4 (Junction)	Reverse
H	5'GTCACTCCATCCACTGTCTCC 3'	4	Reverse
I	5' ATTCTTCGGCCTGAGTAACTG 3'	2	Forward
J	5' GTCATTTCTGTCTCTAGGCTCC 3'	3	Reverse
K	5' ACCCTGCTTCGGTGTCG 3'	2	Forward
L	5' AGCCTTCCTGCCTGGTAA 3'	3	Reverse
M	5' CATTCTTTCCTGGTCTCACTCC 3'	3	Reverse
N	5' GACTTTCCTTTTCCACGACCATC 3'	3	Reverse
O	5' GCTCTGCCAATTGACTTTCC 3'	3	Reverse
S	5'TCAGAAGCCTTTTTCACATAGC 3'	2 and 3 (Junction)	Forward

SUPPLEMENTAL TABLE 3: *CCR2-specific primers, including their assigned letter, exon location, and forward or reverse nature.*

Variants	Label	Sequence	Count	Base Pairs
3	CN	CACCATCATGATTGTTTACTTTCTCTTCTGGACTCCCTATAATATTGTCATTCTCCTGAACACCTTCCAGGAATTCTTCGGCCTGAGTAACTGTGAAAGCACCAGTCAACTGGAC CAAGCCACGCAGGTGACAGAGACTCTTGGGATGACTCACTGCTGCATCAATCCCATCATCTATGCCTTCGTTGGGGAGAAGTTCAGAAGCCTTTTTCACATAGCTCTTGGCTG TAGGATTGCCCCACTCCAAAAACCAGTGTGTGGAGGTCCAGGAGTGAGACCAGGAAAGAATGTGAAAGTGACTACACAAGGACTCCTC	3770	316
		CACCATCATGATTGTTTACTTTCTCTCCTGGACTCCCTATAATATTGTCATTCTCCTGAACACCTTCCAGGAGTGAGACCAGGAAAGAATGTGAAAGTGACTACACGAGGACTC CTC	7336	117
		CACCATCATGATTGTTTACTTTCTCTTCTGGACTCCCTATAATATTGTCATTCTCCTGAACACCTTCCAGGAGTGAGACCAGGAAAGAATGTGAAAGTGACTACACAAGGACTC CTC	4036	117
2	IN	TGAAAGCACCAGTCAACTGGACCAAGCCACGCAGGTGACAGAGACTCTTGGGATGACTCACTGCTGCATCAATCCCATCATCTATGCCTTCGTTGGGGAGAAGTTCAGAAGC CTTTTTCACATAGCTCTTGGCTGTAGGATTGCCCCACTCCAAAAACCAGTGTGTGGAGGTCCAGGAGTGAGACCAGGAAAGAATGTGAAAGTGACTACACAAGGACTCCTC	9670	223
		TGAAAGCACCAGTCAACTGGACCAAGCCACGCAGGTGACAGAGACTCTTGGGATGACTCACTGCTGCATCAATCCCATCATCTATGCCTTCGTTGGGGAGAAGTTCAGAAGCC TTTTTCACATAGCTCTTGGCTGTAGGATTGCCCCACTCCAAAAACCAGTGTGTGGAGGTTCAGGAGTGAGACCAGGAAAGAATGTGAAAGTGACTACACAAGGACTCCTC	3060	223
1	CD	CACCATCATGATTGTTTACTTTCTCTTCTGGACTCCCTATAATATTGTCATTCTCCTGAACACCTTCCAGGAATTCTTCGGCCTGAGTAACTGTGAAAGCACCAGTCAACTGGAC CAAGCCACGCAGGTGACAGAGACTCTTGGGATGACTCACTGCTGCATCAATCCCATCATCTATGCCTTCGTTGGGGAGAAGTTCAGAAGCCTTTTTCACATAGCTCTTGGCTG TAGGATTGCCCCACTCCAAAAACCAGTGTGTGGAGGTCCAGGAGTGAGACCAGGAAAGAATGTGAAAGTGACTACACAAGGACTCCTCGATGGTCGTGGAAAAGGAAAGT CAATTGGCAGAGCCCCTGAAGCCAGTCTTCAGGACAAAGAAGGAGCCTAGAGACAGAAATGACAGATCTCTGCTT	8827	413
1	CJ	CACCATCATGATTGTTTACTTTCTCTTCTGGACTCCCTATAATATTGTCATTCTCCTGAACACCTTCCAGGAATTCTTCGGCCTGAGTAACTGTGAAAGCACCAGTCAACTGGAC CAAGCCACGCAGGTGACAGAGACTCTTGGGATGACTCACTGCTGCATCAATCCCATCATCTATGCCTTCGTTGGGGAGAAGTTCAGAAGCCTTTTTCACATAGCTCTTGGCTG TAGGATTGCCCCACTCCAAAAACCAGTGTGTGGAGGTCCAGGAGTGAGACCAGGAAAGAATGTGAAAGTGACTACACAAGGACTCCTCGATGGTCGTGGAAAAGGAAAGT CAATTGGCAGAGCCCCTGAAGCCAGTCTTCAGGACAAAGAA	11502	379
1	CM	CACCATCATGATTGTTTACTTTCTCTTCTGGACTCCCTATAATATTGTCATTCTCCTGAACACCTTCCAGGAATTCTTCGGCCTGAGTAACTGTGAAAGCACCAGTCAACTGGAC CAAGCCACGCAGGTGACAGAGACTCTTGGGATGACTCACTGCTGCATCAATCCCATCATCTATGCCTTCGTTGGGGAGAAGTTCAGAAGCCTTTTTCACATAGCTCTTGGCTG TAGGATTGCCCCACTCCAAAAACCAGTGTGTGGAGGTCCA	8654	268
1	CO	CACCATCATGATTGTTTACTTTCTCTTCTGGACTCCCTATAATATTGTCATTCTCCTGAACACCTTCCAGGAATTCTTCGGCCTGAGTAA	7863	331
2	ID	TGAAAGCACCAGTCAACTGGACCAAGCCACGCAGGTGACAGAGACTCTTGGGATGACTCACTGCTGCATCAATCCCATCATCTATGCCTTCGTTGGGGAGAAGTTCAGAAGC CTTTTTCACATAGCTCTTGGCTGTAGGATTGCCCCACTCCAAAAACCAGTGTGTGGAGGTCCAGGAGTGAGACCAGGAAAGAATGTGAAAGTGACTACACAAGGACTCCTCG ATGGTCGTGGAAAAGGAAAGTCAATTGGCAGAGCCCCTGAAGCCAGTCTTCAGGACAAAGAAGGAGCCTAGAGACAGAAATGACAGATCTCTGCTT	22228	320
		TGAAAGCACCAGGAGTGAGACCAGGAAAGAATGTGAAAGTGACTACACAAGGACTCCTCGATGGTCGTGGAAAAGGAAAGTCAATTGGCAGAGCCCCTGAAGCCAGTCTTC AGGACAAAGAAGGAGCCTAGAGACAGAAATGACAGATCTCTGCTT	1192	156
1	IJ	TGAAAGCACCAGTCAACTGGACCAAGCCACGCAGGTGACAGAGACTCTTGGGATGACTCACTGCTGCATCAATCCCATCATCTATG	15652	286
1	IL	TGAAAGCACCAGTCAACTGGACCAAGCCACGCAGGTGACAGAGACTCTTGGGATGACTCACTGCTGCATCAATCCCATCATCTATG	13526	381
1	IM	TGAAAGCACCAGTCAACTGGACCAAGCCACGCAGGTGACAGAGACTCTTGGGATGACTCACTGCTGCATCAATCCCATCATCTATG	37647	175
3	IO	TGAAAGCACCAGTCAACTGGACCAAGCCACGCAGGTGACAGAGACTCTTGGGATGACTCACTGCTGCATCAATCCCATCATCTATG	26593	238
		TGATTTTAACCAGGGTTATGTTTTGCAGGAGACTAGGATAGAAAGAGGAGAGAGGCAAGTAGAGTAACCACAACAGTGGACCAAGCAGATAAGGTGAGTAAAGTGGAAAG TTAGACTACACAGGGCATTAAT	5935	132
		TGATTTTAACCAGGGTTGTGTTTTGCAGGAGACTAGGATAGAAAGAGGAGAGAGGCAAGTAGAGTAACCACAACAGTGGACCAAGCAGATAAGGTGAGTAAAGTGGAAA GTTAGACTACACAGGGCATTAAT	3148	132

SUPPLEMENTAL TABLE 4: *Amplicon sequence variant (ASV) table of major sequences, with the count noting how many times the sequence appeared within the PCR product sample for each primer pair. The number of variants for each primer pair may indicate significant variability, or single polynucleotide polymorphisms (SNPs). For example, the second and third CN variants are listed separately despite being the same length and having near-identical sequences because of a point mutation at the 27th base pair, where C has been changed to a T. Similarly, the second variant of IN is a couple base pairs different from the first listed sequence.*